First-principles of wurtzite ZnO (0001) and (000$\bar{1}$) surface structures*

Zhang Yufei(张宇飞), Guo Zhiyou(郭志友)†, Gao Xiaoqi(高小奇), Cao Dongxing(曹东兴), Dai Yunxiao(戴云宵), and Zhao Hongtao(赵洪涛)

(Institute of Optoelectronic Material and Technology, South China Normal University, Guangzhou 510631, China)

Abstract: The surface structures of wurtzite ZnO (0001) and (000$\bar{1}$) surfaces are investigated by using a first-principles calculation of plane wave ultra-soft pseudo-potential technology based on density functional theory (DFT). The calculated results reveal that the surface energy of ZnO–Zn is bigger than that of ZnO–O, and the ZnO–Zn surface is more unstable and active. These two surfaces are apt to relax inward, but the contractions of the ZnO–Zn surface are smaller than the ZnO–O surface. Due to the dispersed Zn4s states and the states of stronger hybridization between the Zn and O atoms, the ZnO–Zn surface shows n-type conduction, while the O2p dangling-bond bands in the upper part of the valence cause the ZnO–O surface to have p-type conduction. The above results are broadly consistent with the experimental results.

Key words: ZnO (0001) and (000$\bar{1}$); surface energy; surface relaxation; electronic structures
DOI: 10.1088/1674-4926/31/8/082001 **PACC:** 6820; 6810C; 7320A

1. Introduction

The study of solid surfaces is an indispensable subdiscipline of materials research since a solid sample is always in contact with other media via its surface[1]. A microscopic determination of semiconductor surface structure is crucial in understanding its material properties and can provide important guidance to modulate material properties during crystal growth. ZnO is one of the wide-bandgap semiconductors, and has attracted much attention due to its great usage in a variety of sensor and optoelectronic applications and the fairly low cost for high-quality bulk material[2]. *c*-axis ZnO has two distinct polar surfaces: Zn-polar (0001) and O-polar (000$\bar{1}$) surfaces. During crystal growth, the difference in polarity between these two faces affects the growth mode, impurity incorporation, and dislocation formation[3]. Recently, many experimental and theoretical investigations on *c*-axis polar ZnO surfaces have been reported: low-energy electron diffraction measurements have revealed that both Zn-polar (0001) and O-polar (000$\bar{1}$) surfaces exhibit (1 × 1) patterns[4, 5], suggesting that these polar surfaces are bulk terminated; Dulub *et al.*[6] proposed from a scanning tunneling microscopy (STM) study combined with *ab initio* calculations that the formation of pits and islands was essential to stabilize the Zn-polar (0001) surface; angle-resolved photoelectron spectroscopy (ARPES)[7] and electron-counting rule (ECR) study[8] have elucidated the stabilization mechanism of the *c*-axis ZnO polar surfaces. As far as we know, the existence of the (1 × 1) terminated Zn-polar (0001) and O-polar (000$\bar{1}$) surface has been probed, but very few systematical studies on how the electronic structures of the polar surfaces are affected by surface termination have been reported. In this paper, we will investigate the electronic properties of wurtzite ZnO (0001) and (000$\bar{1}$) surfaces by means of a first-principles calculation.

2. Theoretical approaches

The present calculations are based on density-functional theory (DFT) within the generalized gradient approximation (GGA)[9] which is parametrized by Perdew, Burke, and Ernzerhof (PBE)[10] using the plan-wave pseudo-potential method. The wave functions are expanded in a plane-wave basis with a cutoff energy of 400 eV. We first optimize the bulk wurtzite ZnO structure, yielding the following lattice parameters: a = 3.2844 Å, c = 5.2901 Å. These lattice parameters are in very good agreement with the experiment results[11], a = 3.2496 Å and c = 5.2042 Å.

For the surface calculations, our supercells contain six (0001) bilayers in which the lower four bilayers are fixed as the bulk configuration while the upper two bilayers and adatoms (or adlayers) are allowed to relax. Figure 1 shows the schematic structures of *c*-axis ZnO polar surfaces, where each anion is surrounded by four cations at the corners of a tetrahedron, and vice versa. The tetrahedral coordination is typically of sp^3 covalent bonding, but these materials have a substantial ionic characteristic. To prevent unphysical charge transfer between the top and bottom slab surfaces, pseudohydrogens with fractional charges are used. A 3 × 3 × 1 Monkhorst–Pack mesh[12] is used for the Brillouin zone integration. The structural optimization is terminated when the magnitude of the Hellmann–Feynman force on each ion is less than 0.03 eV/ Å. We perform calculations with vacuum thicknesses of 12.5 Å and 13.8 Å. The two sets of calculations yield almost identical results. Therefore we present the results in the case of the vacuum thickness of 12.5 Å.

* Project supported by the National Natural Science Foundation of China (No. 60877069) and the Research Project of Science and Technology of Guangzhou, Guangdong Province, China (Nos. 2007A010500011, 2008B010200041).
† Corresponding author. Email: guozy@scnu.edu.cn
Received 10 December 2009, revised manuscript received 30 March 2010

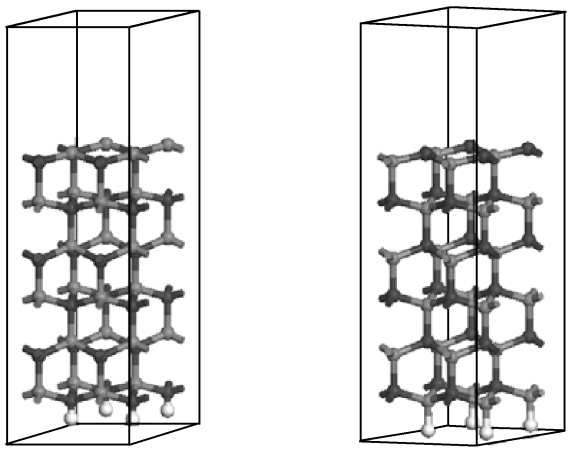

(a) (b)

Fig. 1. Three-dimensional views of the upper part of (a) the perfect (0001) surface, and (b) the $(000\bar{1})$ surface. The black and the gray are O and Zn atoms, respectively. Four pseudohydrogen atoms (shown as white balls) are found at the bottom of the cell.

Table 1. Surface energies of 8-slab and 12-slab ZnO $(000\bar{1})$ and (0001) surfaces.

Surface slab	Surface energy (eV/m^2)	
	ZnO:Zn-polar (0001)	ZnO:O-polar $(000\bar{1})$
8	2.2838	2.2738
12	1.9365	1.8981

3. Results and discussion

3.1. Surface energy

For the perfect surface and a 1 × 1 unit cell, the surface energy which corresponds to the energy variation due to the creation of a surface is given by the relation as follows[13–15]:

$$E_{\text{surf}}(n,l) = \frac{E_{\text{slab}}(n,\ l) - E_{\text{bulk}}(n,\ 0)}{A_{\text{slab}}}. \qquad (1)$$

Here, $E_{\text{slab}}(n,l)$ and $E_{\text{bulk}}(n,0)$ are the total energies of the unit cell for an n-layer slab (a cell with a vacuum thickness of l) and the corresponding bulk (a cell without vacuum), respectively. A_{slab} is the total area of the surface considered. For material slab models, the smaller the surface energy is, the more stable the surface is. The reason for this is that the surface with a higher surface energy promotes adhesion and spreading of a cell[16, 17].Our calculated surface energies are shown in Table 1; the surface energies of the 8-layer and 12-layer slab models reflect that the relative error is very small. By comparison, we found that the surface energy of the Zn-polar (0001) surface is bigger than that of the O-polar $(000\bar{1})$ surface, which shows that the ZnO–Zn surface is more active than the ZnO–O surface. This is in good agreement with the experimental report that triangular shaped pits and islands which are active regions for adsorption are formed on the ZnO–Zn surface, while the ZnO–O one is characterized by smooth terraces with a considerably lower step density[6, 18].

Table 2. Relaxation of the distance between the uppermost four layers.

Interlayer relaxation	ZnO–Zn surface		ZnO–O surface	
	GGA	LDA	GGA	LDA
R_{12} (Å)	–0.109	0.002	–0.301	–0.393
R_{23} (Å)	0.136	0.154	0.112	0.031
R_{34} (Å)	–0.041	–0.087	–0.083	–0.101

3.2. Surface geometric relaxation

In order to remove the surface atomic force added on ZnO–Zn and ZnO–O surfaces, we keep the positions of other inner atoms unchanged and optimize the atomic structures of the two surfaces. Before we proceed to present the properties of ZnO surface structures, we first compare the results of our calculations within the GGA as parametrized by PBE and the local density approximation (LDA) as parametrized by Perdew-Zunger[19]. DFT within the local density approximation (LDA)[20, 21] is the standard approach for calculating the electronic and structural properties that are the focus of the present investigation at present. In general, for calculations of lattice constant in semiconductors within the DFT approach, using the LDA seems to be well justified[22]. LDA is a class of approximations to the exchange-correlation (XC) energy functional in DFT that depend solely upon the value of the electronic density at each point in space. To verify the reliability of the data, we calculate the same surface structure with these two different methods via the GGA and the LDA, respectively.

The calculated results for two surfaces are listed in Table 2. The relaxed results of the distance between the uppermost four layers (R12, R23, R34) are given by way of the difference from the unrelaxed ideal interlayer distance. The distances between the first double layer and outer four layers are calculated to be –0.189 Å and –0.272 Å for the ZnO–O surface, in good agreement with the experimental results of –0.2 Å[23] and –0.3 Å[24], meanwhile, the contraction of the outer four layers of the ZnO–Zn surface is much smaller with a value of –0.013 Å, which is close to the experimental result[25].

We can see that both polar surfaces tend to relax inward, but the contraction of the ZnO–Zn surface is much smaller than that of the ZnO–O surface. Because surface relaxation is mainly affected by Coulomb force and hybrid quantum effect, four ligands of the surface Zn atoms (or O atoms) turn into three ligands, and each surface atom has a dangling bond, which will lead to the recombination of atomic orbitals of the surface. Due to the different electronegativities of the surface atoms, surface dangling bonds are prone to electronic transferring, resulting in the enhancement of cation–anion Coulomb force and surface contraction.

3.3. Electronic structures

The electronic structures of the ZnO–Zn and ZnO–O surfaces are affected by surface termination. These polar surfaces have the same bulk structure, but they have different atomic compositions and different surface morphologies. Surface states are electronic states of the surfaces of materials. They are formed due to the sharp transition from solid material that ends with a surface and are found only at the atom layers closest to the surface. The termination of a material with a surface leads to a change of the electronic band structure from the

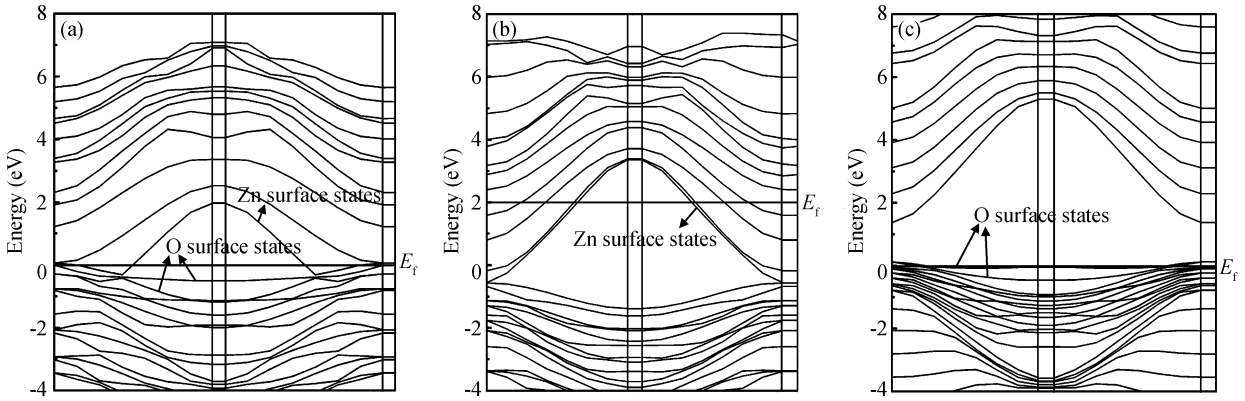

Fig. 2. Band structures of six (1 × 1) wurtzite bilayers of (a) a pristine ZnO {0001} film, (b) a ZnO–Zn surface with the opposite O surface layer passivated with pseudohydrogens, and (c) a ZnO–O surface with the opposite Zn surface layer passivated with pseudohydrogens. O surface states in (b) and Zn surface states in (c) were moved away from E_f by the passivation. The surface states in (b) and (c) remain the same as the ones in the clean ZnO surface case when the opposite surface is pseudohydrogen passivated.

bulk material to the vacuum. In the weakened potential at the surface, new electronic states can be formed, which are surface states. In this article, the nature of surface states has been investigated by comparing the surface band structures with and without pseudohydrogen saturation. When one of the two polar surfaces of ZnO films is passivated with pseudohydrogens, the corresponding surface band structure can be obtained, then comparing it with the ones of which neither of the surfaces are passivated we can distinguish between Zn and O surface states and get the nature of surface states of the other surface without passivation.

To study the surface states of the polar surface films, we have passivated only one surface at a time, that is, either the ZnO–Zn surface or ZnO–O surface is passivated, to compare with ZnO films, of which neither O nor Zn terminated surfaces are passivated. For instance, in Fig. 2(b), only the O surface is passivated with pseudohydrogens to study Zn surface states at E_f. The polar surface study is based on the fact that even when only one surface is passivated with pseudohydrogens, the band structure (except surface states) is similar to the bulk band structure, which suggests that the extra electric field due to the dipole structure was significantly reduced. As can be seen in Figs. 2(a) and 2(b), we find that the unoccupied ZnO–Zn surface states at E_f remain exactly the same when the ZnO–O surface states are moved away from E_f due to the passivation. The same explanation can be applied to the ZnO–O surface when only the ZnO–Zn surface is passivated, as in Fig. 2(c). Thus, we can make sure of the positions of the ZnO–Zn and ZnO–O surface states and then study them. Here, the ZnO–Zn and ZnO–O surface states are situated at the bottom of the conduction band and the top of the valence band, respectively. Compared to the band structure of clean ZnO films as shown in Fig. 2(a), on the one hand the band structure of the ZnO–Zn surface declines a lot as a whole relative to the Fermi level and the ZnO–Zn surface states become steeper, while on the other hand the band structure of the ZnO–O surface rises a little as a whole relative to Fermi level and the ZnO–O surface states become flatter, but the valence bands dramatically change. At the same time, the small occupation near Γ should be noticed.

In order to evaluate the effect that the structure termination has on the electronic structure, the band structures are calculated and compared in Fig. 3. For the ZnO–Zn surface, a narrow surface band gap about 0.22 eV exists above the top of the valence band. In addition, the Fermi level enters into the conduction band deeply, and partial surface states appear below the Fermi level. Therefore, the ZnO–Zn surface is of n-type conduction characteristic. Completely different from the ZnO–Zn surface, the ZnO–O surface has a surface band gap about 1.04 eV, and the Fermi level shifts into the valence band, which predicts that the ZnO–O surface has p-type conduction behavior. The calculated results are in good agreement with the theory and the experiment[26, 27].

The ambient environment of surface atoms commonly affects the local atomic states of two or three outer bilayers in the slab model. In general, surface states exist near E_f due to their nonbonding characteristic[28, 29] and the charge distribution near the surface is distorted due to the broken translational symmetry and the vacuum. Now, Figures 2 and 4 clearly demonstrate that the ZnO–Zn and ZnO–O surface states indeed appear near the band gap with a relatively large density of states. The farther it goes into the inside, the less influence the electronic states of atoms will get from the surface environment, and the weaker the peak associated with the surface states will be. Thus, the orbital characteristics of the surface states can be differentiated by the partial local density of states[30]. Figure 4 shows the partial densities of the ZnO–Zn and ZnO–O surfaces, which were calculated to illustrate the contributions of different atoms to the surface states. According to the partial densities of states as shown in Fig. 4(a), the ZnO–Zn surface states are mainly derived from the Zn4s states of the first double layer due to the strong hybridization between the Zn and O atoms, and the O2p states also make a contribution. However, such O2p states are mainly from the first double layer, and those from other double layers inside make almost no contribution. Ranging from –2 to 0 eV, the surface states are filled with Zn4s and O2p states. Because of the ZnO–Zn surface characteristics, the Fermi level enters the conduction band, which is accompanied by the formation of surface states. Above the Fermi level, although the distribution of the Zn and O atoms is almost indistinguishable from 0.5 to 1.2 eV, the surface states have a peak in the vicinity of 1.86 eV, which can help us distinguish the Zn4s and O2p states.

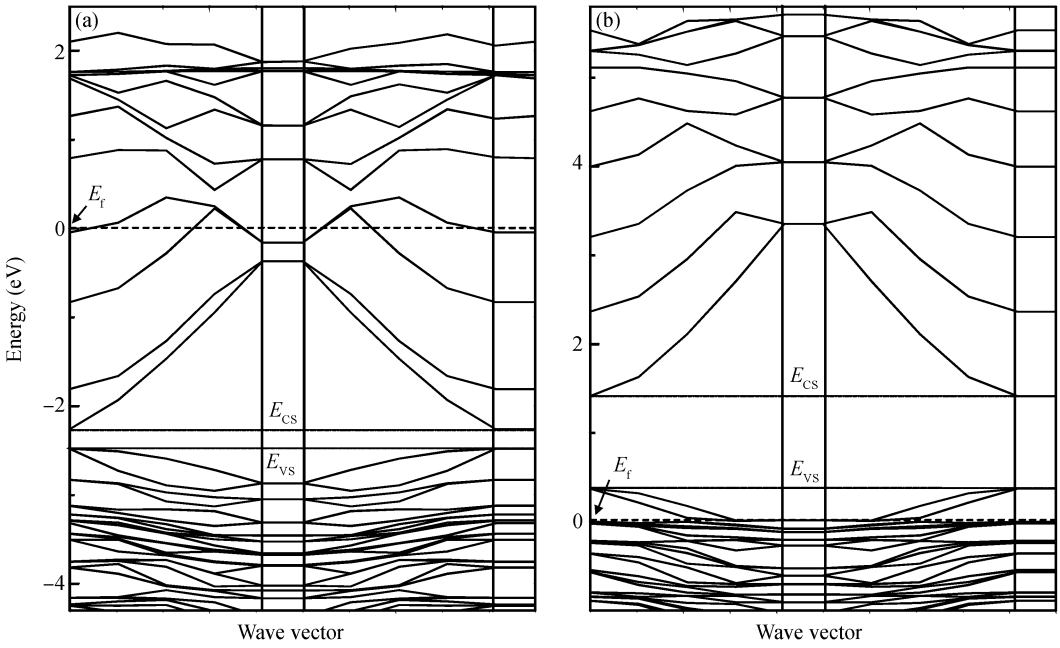

Fig. 3. Energy band structures of (2 × 2) ZnO–Zn (a) and ZnO–O (b) surfaces. The Fermi level is situated at 0 eV and is indicated by the arrow. The top of the valence band and the bottom of the conduction band of both polar surfaces are marked by dash dotted lines and denoted as E_{VS} and E_{CS}, respectively.

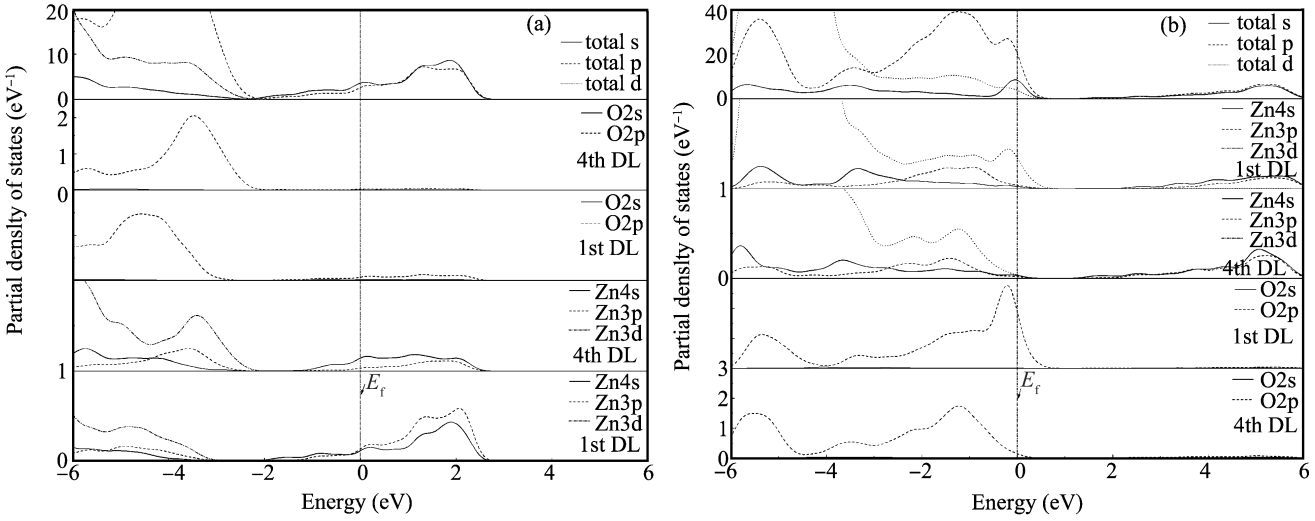

Fig. 4. Partial densities of states of Zn and O atoms of the first double layer (DL) and the fourth double layer are plotted for ZnO–Zn (a) and ZnO–O (b) surfaces. The Fermi level is situated at 0 eV and is denoted by an arrow.

Regarding the ZnO–O surface states shown in Fig. 4(b), due to the strong hybridization between Zn and O atoms, the Zn3d and O2p states derived from the first double layer show a peak at –0.2 eV while the Zn3d and O2p states from the fourth layer show a peak at –1.23 eV. The surface states above the Fermi level are mainly derived from the Zn and O atoms in the first double layer. Nevertheless, the surface states above the Fermi level are discrete because the surface band gap interrupts the continuity. The ZnO–O surface states are formed in the valence band where the Fermi level shifts down a little from the top of the valence band. That is to say, the ZnO–O surface shows p-type conductivity. By comparing the densities of states of the ZnO–Zn and ZnO–O surface, we find that n-type conductivity of the ZnO–Zn surface and p-type conductivity of the ZnO–O surface are attributable to the Zn and O dangling-bond bands in the lower part of the conduction band and the upper part of the valence band[31, 32] which cause the surface states to distribute in the conduction band and the valence band, respectively.

4. Conclusions

We have performed density functional theory calculations to determine the structure properties of wurtzite ZnO (0001) and (000$\bar{1}$) surfaces. We consider the surface energies of these two distinct polar surfaces and find that the surface energy of Zn-polar (0001) is bigger than that of O-polar (000$\bar{1}$). That is to say, the ZnO–Zn surface is more unstable and active than the

ZnO–O surface. The geometric relaxation calculations show that both the distinct polar surfaces are apt to relax inward, but the contractions of the ZnO–Zn surface are much smaller than those of the ZnO–O surface.

We have investigated the nature of surface states by comparing the surface band structures with and without pseudohydrogen saturation, finding that the ZnO–Zn and ZnO–O surface states are situated at the bottom of the conduction band and the top of the valence band respectively, and the band structures of the two polar surfaces with H saturation change greatly compared to the one without H saturation. Partial densities of states of Zn and O atoms in different double layers tell us that the surface states are mainly attributed to the first double layer atoms. For the (0001) surface, we find that the Fermi level enters the conduction band deeply, which cause the n-type conduction of the ZnO–Zn surface as a result of the dispersed Zn4s states and the states of stronger hybridization between the Zn and O atoms. For the ZnO–O surface, the O2p dangling-bond bands lie in the upper part of the valence and the Fermi level shifts down a little into the valence band, which shows that the ZnO–O surface tends to the p-type conduction characteristic.

References

[1] Bechstedt F. Principles of surface physics. Berlin: Springer, 2003: 1

[2] Moore J C, Kenny S M, Baird C S, et al. Electronic behavior of the Zn- and O-polar ZnO surfaces studied using conductive atomic force microscopy. J Appl Phys, 2009, 105: 116102

[3] Kato H, Sano M, Miyamoto K, et al. Polarity control of ZnO on *c*-plane sapphire by plasma-assisted MBE. J Cryst Growth, 2005, 275: 2459

[4] Dulub O, Boatner L A, Diebold U. STM study of the geometric and electronic structure of ZnO (0001)-Zn, $(000\bar{1})$-O, $(10\bar{1}0)$, and $(11\bar{2}0)$ surfaces. Surf Sci, 2002, 519: 201

[5] Lindsay R, Muryn C A, Michelangel E, et al. ZnO (0001)-O surface structure: hydrogen-free (1×1) termination. Surf Sci, 2004, 565: L283

[6] Dulub O, Diebold U, Kresse G. Novel stabilization mechanism on polar surfaces: ZnO (0001)-Zn. Phys Rev Lett, 2003, 90: 016102

[7] Ozawa K, Oba Y, Edamoto K, et al. Valence-band structure of the polar ZnO surfaces studied by angle-resolved photoelectron spectroscopy. Phys Rev B,2009, 79: 075314

[8] Du M H, Zhang S B, Northrup J E, et al. Stabilization mechanisms of polar surfaces: ZnO surfaces. Phys Rev B,2008, 78: 155424

[9] Payne M C, Teter M P, Allan D C, et al. Iterative minimization techniques for *ab initio* total-energy calculations: molecular dynamics and conjugate gradients. Rev Mod Phys, 1992, 64: 1045

[10] Perdew J P, Burke K, Ernzerhof M. Generalized gradient approximation made simple. Phys Rev Lett, 1996, 77: 3865

[11] Karzel H, Potzel W, Köfferlein M, et al. Lattice dynamics and hyperfine interactions in ZnO and ZnSe at high external pressures. Phys Rev B, 1996, 53: 11425

[12] Monkhorst H J, Pack J D. Special points for Brillouin-zone integrations—a reply. Phys Rev B, 1977, 16: 1748

[13] Ramamoorthy M, Vanderbilt D, King-Smith R D. First-principles calculations of the energetics of stoichiometric TiO_2 surfaces. Phys Rev B, 1994, 49: 16721

[14] Bates S P, Kresse G, Gillan M J. A systematic study of the surface energetics and structure of TiO_2 (110) by first-principles calculations. Surf Sci, 1997, 385: 386

[15] Fiorentini V, Methfessel M. Extracting convergent surface energies from slab calculations. J Phys: Condens Matter, 1996, 8: 6525

[16] Song D P, Liang Y C, Chen M J, et al. Molecular dynamics study on surface structure and surface energy of rutile TiO_2 (110). Appl Surf Sci, 2009, 255: 5702

[17] Redey S A, Razzouk S, Rey C, et al. Osteoclast adhesion and activity on synthetic hydroxyapatite, carbonated hydroxyapatite, and natural calcium carbonate: relationship to surface energies. J Biomed Mater Res, 1999, 45: 140

[18] Ostendorf F, Torbrügge S, Reichling M. Atomic scale evidence for faceting stabilization of a polar oxide surface. Phys Rev B, 2008, 77: 041405

[19] Perdew J P, Zunger A. Self-interaction correction to density-functional approximations for many-electron systems. Phys Rev B, 1981, 23: 5048

[20] Hohenberg P, Kohn W. Inhomogeneous electron gas. Phys Rev, 1964, 136: B864; Kohn W, Sham L J. Self-consistent equations including exchange and correlation effects. Phys Rev, 1965, 140: A1133

[21] Ceperley D M, Alder B J. Ground state of the electron gas by a stochastic method. Phys Rev Lett, 1980, 45: 566

[22] Stampfl C, van de Walle C G. Density-functional calculations for III–V nitrides using the local-density approximation and the generalized gradient approximation. Phys Rev B, 1999, 59: 5521

[23] Jedrecy N, Gallini S, Sauvage-Simkin M, et al. Copper growth on the O-terminated ZnO $(000\bar{1})$ surface: structure and morphology. Phys Rev B, 2001, 64: 085424

[24] Jedrecy N, Sauvage-Simkin M, Pinchaux R. The hexagonal polar ZnO (0001)-(1×1) surfaces: structural features as stemming from X-ray diffraction**.** Appl Surf Sci, 2000, 162/163: 69

[25] Sambi M, Granozzi G, Rizzi G A, et al. An angle-scanned photoelectron diffraction study on the surface relaxation of ZnO (0001). Surf Sci, 1994, 319: 149

[26] Zhou C J, Kang J Y. Electronic structures of ZnO (0001)-Zn and $(000\bar{1})$-O polar surfaces. J Mater Sci: Mater Electron, 2008, 19: S229

[27] Urbieta A, Fernandez P, Hardalov C, et al. Cathodoluminescence and scanning tunnelling spectroscopy of ZnO single crystals. Mater Sci Eng B, 2002, 91/92: 345

[28] Shockley W. On the surface states associated with a periodic potential. Phys Rev, 1939, 56: 317

[29] Posternak M, Krakauer H, Freeman A J, et al. Self-consistent electronic structure of surfaces: surface states and surface resonances on W (001). Phys Rev B, 1980, 21: 5601

[30] Li Y H, Xu P H, Pan H B, et al. First-principle study on GaN (1010) surface structure. Acta Phys Sin, 2005, 54: 0317

[31] Wander A, Schedin F, Steadman P, et al. Stability of polar oxide surfaces. Phys Rev Lett, 2001,86: 3811

[32] Kresse G, Dulub O, Diebold U. Competing stabilization mechanism for the polar ZnO (0001)-Zn surface. Phys Rev B, 2003, 68: 245409